Journal of Thermal Analysis and Calorimetry, Vol. 81 (2005) 111–118

SYNTHESIS, SPECTRAL AND THERMAL CHARACTERIZATION OF 6-HYDROXYMETHYL PYRIDINE-2-CARBOXYLIC ACID METHYL ESTER AND ITS COMPLEXES

Nadia E. A. El-Gamel and G. G. Mohamed[*]

Chemistry Department, Faculty of Science, Cairo University, Giza, Egypt

New pincer ligand, 6-hydroxymethylpyridine-2-carboxylic acid methyl ester, HL, and its bipositive, tripositive and uranyl metal complexes have been synthesized and characterized by elemental and thermal analyses, IR, diffuse reflectance and ^{1}H NMR spectra, molar conductance and magnetic moment measurements. The downfield shift of the aliphatic OH signal (from 3.87 *vs.*2.96 ppm in the ligand) upon complexation indicates the coordination by protonated aliphatic OH group. Zn(II) and UO_2(II) complexes are found to be diamagnetic as expected. The low molar conductance values indicate that Ni(II) and Zn(II) complexes are non electrolytes; Fe(II), Co(II), Cu(II) and UO_2(II) complexes are 1:2 electrolytes while Fe(III) complex is a 1:3 electrolyte. The general compositions of the complexes are found to be $[M(HL)X_2]\cdot nH_2O$ where M=Ni(II) (X=Cl, n=1) and Zn(II) (X=Br, n=0); and $[M(HL)_2]X_m\cdot nH_2O$ where M=Fe(II) (X=Cl, m=2, n=0), Fe(III) (X=Cl, m=3, n=4), Co(II) (X=Cl, m=2, n=0), Cu(II) (X=Cl, m=2, n=0) and UO_2(II) (X=NO_3, m=2, n=0). The thermal behaviour of the complexes has been studied and different thermodynamic parameters are calculated using Coats–Redfern method.

Keywords: *^{1}H NMR, 6-hydroxymethylpyridine-2-carboxylic acid methyl ester, IR, magnetic moment, metal complexes, molar conductance, solid reflectance, thermal analysis*

Introduction

In many catalytic reactions, coordinatively unsaturated complexes appear as reactive intermediates at some stages. Such species initiate catalytic processes (catalytic precursor) and, of course, are part of catalytic cycles themselves. Thus, investigations of the factors controlling and affecting the reactivity and stability of unsaturated compounds are very important not only for intrinsic reasons but for the understanding of virtually all homogeneously catalyzed processes. Recently, the pincer ligand class (1) has experienced a renaissance [1] from its earliest incarnations in mono-metal coordination chemistry. Here, *E* is a nitrogen or phosphorous donor and *E*` can be either a pyridine nitrogen or ring $sp^2$ carbon as shown in Fig. 1. This ligand is most often found as a meridional ligand (i.e., *E*` and two *E* will be approximately coplanar in the metal coordination sphere).

1 2

Fig. 1 Pincer ligands with *E*=N or P and *E*'=pyridine N or sp^2 ring carbon

A progress on a related goal pincer ligand chemistry of transition metals with a secondary amine donor at site E was reported [1]. Moreover, the donors E was made secondary amine (i.e., NH^tBu) rather than tertiary amines for the specific purpose of having a reactive hydrogen accompanied by a bulky but 3-fold symmetric substituent [1]. This substitution pattern (ligand abbreviation N_2py when *E*`=N) will give rise to both mirror and C_2 asymmetric isomers **3**, which are not anticipated to interconvert on the synthetic time scale when the nitrogens are coordinated. it is shown from Fig. 2 that, isomer 3 (m) clearly has a crowded ('up') and an uncrowded ('down') sides, while in 3(C_2) these are equivalent. The Ru(II)/Cl^-, NCMe, PPh_3 chemistry of the related (but C_{2v} symmetric) ligand 4 was recently reported [2, 3]. 2-tertbutylaminomethylpyridine-6-carboxylic acid methylester ligand and its metal complexes were previously reported by the authors [4]

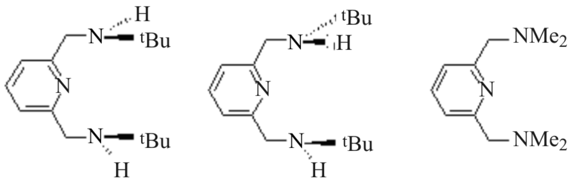

3(m) 3(C_2) 4

Fig. 2 N_2Py ligand with mirror and C_2 asymmetric isomers

---

[*] Author for corresponding: ggenidy@hotmail.com

1388–6150/$ 20.00

Akadémiai Kiadó, Budapest, Hungary
Springer, Dordrecht, The Netherlands

The main idea of this article is to prepare an asymmetric pincer ligand type with *E*` is a nitrogen and *E* as aliphatic OH in one arm and as COOMe in the second arm. The ligand and its complexes were characterized using different physico-chemical tools like elemental and thermal analyses, magnetic moment, molar conductance, IR, ^{1}H NMR and solid reflectance spectral techniques.

Experimental

All reagents and solvents were obtained from commercial sources and used as received. Elemental analyses were carried out at the Microanalytical Center at Cairo University. Infrared spectra were recorded on a Perkin Elmer FT-IR type 1650 spectrophotometer in wavenumber region 4000–200 cm^{-1}. The spectra were recorded as KBr disc. The molar conductance of solid complexes in DMF was measured using Sybron-Barnstead conductometer. The solid reflectance spectra were measured on a Shimadzu 3101 pc spectrophotometer. The molar magnetic susceptibility was measured on powdered samples using the Faraday method. The thermogravimetric analysis (TG and DTG) was carried out in dynamic nitrogen atmosphere (20 cm^3 min^{-1}) with a heating rate of 10°C min^{-1} using Shimadzu TGA-50H thermal analyzer. The ^{1}H NMR spectra were recorded using a Bruker ARX-300 instrument. Chemical shifts are reported in parts per million downfield from tetramethylsilane. Deuterated chloroform and DMSO were used as a solvent in a concentric tube containing d_6-acetone.

2,6-pyridinedicarboxylic acid dimethyl ester ($C_9H_9NO_4$)

2,6-pyridinedicarboxylic acid (26.0 g, 155.7 mmol) and H_2SO_4 concentrated (0.2 cm^3) in methanol (200 cm^3) were heated to reflux for 100 h. After evaporation of the solvent, the residue was redissolved in CH_2Cl_2 (200 cm^3), extracted twice with saturated aqueous solutions of $NaHCO_3$ (100 cm^3) followed by H_2O (100 cm^3). The organic layer was dried over Na_2SO_4, filtered and the solvent removed. The white product was dried in vacuo. Yield: 26.0 g (85%) IR (KBr disc): 1730 sh ($\nu_{C=O}$), 1595 sh ($\nu_{C=N}$), ^{1}H NMR (25°C, $CDCl_3$): δ(ppm)=8.33 (d, 2H, *J*=7.8 Hz), 8.02 (t, 1H, *J*=7.8 Hz), 4.02 (s, 6H).

2-hydroxymethylpyridine-6-carboxylic acid methyl ester ($C_8H_9NO_3$) (HL)

To 2,6-pyridinedicarboxylic acid dimethylester (20.9 g, 107.1 mmol) in MeOH (200 cm^3) was slowly added $NaBH_4$ (10.5 g, 55 mol), whereupon the exothermic reaction warmed the reaction mixture to reflux. The solution was then stirred at room temperature for 12 h. After evaporation of the solvent, the residue was dissolved in saturated aqueous $NaHCO_3$ solution (200 cm^3) and extracted with $CHCl_3$ (300 cm^3) by continuous liquid-liquid extraction for 15 h. After evaporation of the solvent, the white product was washed with Et_2O and dried in vacuo. Yield: 15.0 g (72%) IR (KBr disc): 3384 br (ν_{OH}), 1732 sh ($\nu_{C=O}$), 1590 sh ($\nu_{C=N}$), ^{1}H NMR (25°C, DMSO-d_6): δ (ppm)=7.75 (t, 1H, *J*=7.3 Hz), 7.35 (d, 2H, *J*=7.3 Hz), 4.65 (s, 2H), 2.96 (bs, 1H), 3.94 (5, 3H).

Results and discussion

The HL ligand used in this work is a new ligand, prepared in a similar manner to 2,6-bis (hydroxymethyl) pyridine previously published [5]. The preparation of HL is given in Scheme 1.

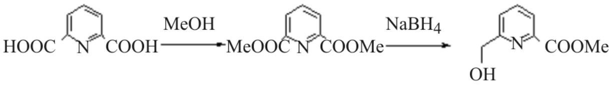

Scheme 1 Preparation of HL ligand.

The ^{1}H NMR spectrum of HL is given in Fig. 3 with indexing of various types of protons. The formation of this ligand is revealed by the appearance of pyridyl protons at 7.75 and 7.35 ppm, $-COOCH_3$ proton at 3.94 ppm, $-CH_2$ protons at 4.65 ppm and OH proton at 2.96 ppm. This is further supported by the appearance of bands due to (C=O), δ(C=N) and (C–O) at 1732, 1590 and 1231 cm^{-1} respectively. All the new complexes have the $[M(HL)X_2]\cdot nH_2O$ (*M*=Ni(II) and Zn(II), *X*=Cl or Br and *n*=0–1) and $[M(HL)_2]X_m\cdot nH_2O$ (*M*=Fe(II) (*X*=Cl, *m*=2, *n*=0), Fe(III) (*X*=Cl, *m*=3, *n*=4), Co(II) (*X*=Cl, *m*=2, *n*=0), Cu(II) (*X*=Cl, *m*=2, *n*=0) and UO_2(II) (*X*=NO_3, *m*=2, *n*=0) stoichiometry and were prepared by reaction of HL with metal salts in ethanol according to the reaction given below:

$$MX_2+HL+nH_2O \rightarrow [M(HL)X_2]\cdot nH_2O$$

$$(M=Ni(II), Zn(II))$$

$$MX_m+2HL+nH_2O \rightarrow [M(HL)_2]X_m\cdot nH_2O \ (M=Fe(II),$$

$$Fe(III), Co(II), Cu(II), UO_2(II))$$

The complexes are insoluble in ethanol, acetone, chloroform, ether, methanol, methylenechloride but have a good solubility in DMF and DMSO. Analytical data, decomposition points and colours of the

Table 1 Analytical and physical data of HL and its complexes

Compound	Colour (yield/%)	*M.p.*/°C	Found (Calcd)/%				$\mu_{eff.}$ (B.M.)	Λ_m/ Ω^{-1} cm^2 mol^{-1}
			C	H	N	M		
HL $C_8H_9NO_3$	white (90)	75	57.32 (57.49)	5.65 (5.39)	8.49 (8.38)	–	–	–
$[Fe(HL)_2]Cl_2$ $C_{16}H_{18}Cl_2FeN_2O_6$	yellow (73)	Dec.	41.90 (41.65)	4.15 (3.90)	5.89 (6.07)	12.40 (12.15)	4.98	193
$Fe(HL)_2]Cl_3\cdot 4H_2O$ $C_{16}H_{26}Cl_3FeN_2O_7$	brown (82)	Dec	33.94 (33.78)	4.22 (4.57)	5.05 (4.93)	10.23 (9.85)	5.30	280
$[Co(HL)_2]Cl_2$ $C_{16}H_{18}Cl_2CoN_2O_6$	rose (80)	Dec.	41.58 (41.38)	4.00 (3.88)	6.32 (6.03)	12.51 (12.72)	5.15	185
$Ni(HL)Cl_2]\cdot H_2O$ $C_8H_{11}Cl_2NNiO_4$	green (62)	Dec.	30.80 (30.38)	3.69 (3.48)	4.82 (4.43)	18.73 (18.99)	3.32	13.75
$Cu(HL)_2]Cl_2$ $C_{16}H_{18}Cl_2CuN_2O_6$	yellow (69)	Dec.	40.58 (40.98)	3.79 (3.84)	5.63 (5.98)	13.90 (13.55)	1.95	188
$[Zn(HL)Br_2]$ $C_8H_9Br_2NO_3Zn$	white (80)	Dec.	24.25 (24.49)	2.44 (2.30)	3.42 (3.57)	16.32 (16.58)	diam.	21.42
$[UO_2(HL)_2](NO_3)_2$ $C_{16}H_{18}N_4O_{14}U$	yellow (76)	Dec.	26.79 (26.52)	2.71 (2.49)	8.09 (7.37)	–	diam.	202

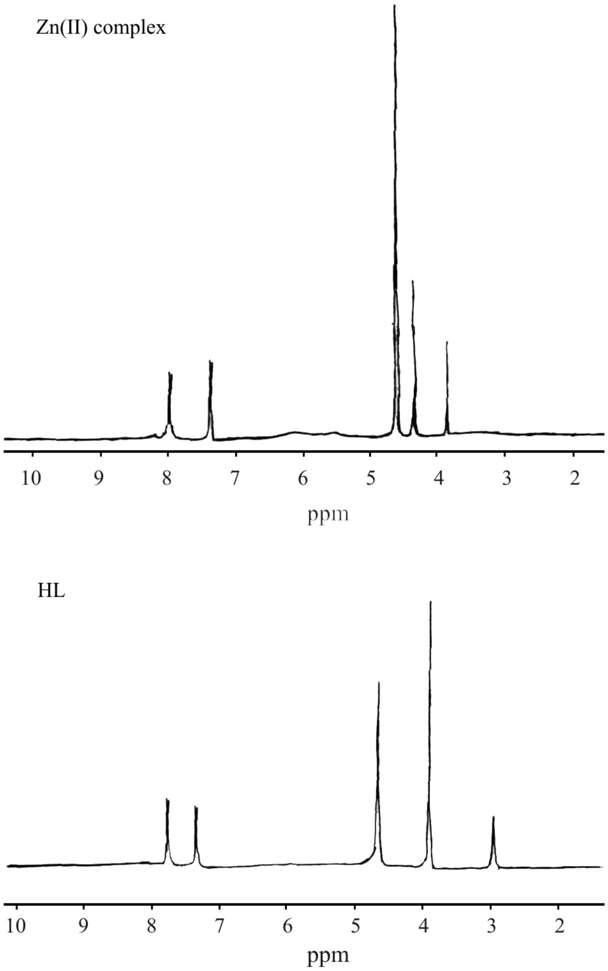

Fig. 3 ^{1}H NMR spectra of HL and its Zn(II) complex

complexes are shown in Table 1. They are characterized by the following physicochemical studies.

IR spectra and mode of bonding

The effective IR spectral bands of the ligand and its metal complexes with Fe(III), Co(II), Ni(II), Cu(II) and Zn(II) and UO_2(II) are listed in Table 2 together with assignments for most of the major peaks. The ligand used in the present investigation contains three possible donor sites: (*i*) aliphatic OH, (*ii*) pyridyl nitrogen and (*iii*) carboxylate oxygen.

The ν(C=N) band occurs at 1590 cm^{-1} in the free ligand. This band shifts to higher frequency by 9–49 cm^{-1} after complexation, indicating the coordination of pyridyl nitrogen to metal ions [6]. The participation of the pyridyl nitrogen; as its band overlapped with those of the carboxylate group, is confirmed from the band due to in-plane deformation ρ(py) located at 667 cm^{-1} in the free ligand. The coordination of the pyridyl nitrogen to the metal ions is confirmed by the blue shift (47 cm^{-1}) or red shift (2–23 cm^{-1}) of the ρ(py) [7–9]. In the wavenumber region 1732 cm^{-1} range, some of the most characteristic bands of these systems are found. The so-called amide I band, which represents mainly the ν(C=O) stretching mode, in the chelates. This band is shifted to higher frequency (6–48 cm^{-1}), supporting the participation of the carbonyl group of this ligand in the metal coordination [10]. The bands at the wavenumber 1573 and 1304 cm^{-1} regions in the free ligand are assigned to the asymmetric and symmetric stretching vibrations of the carboxylate group, respectively. The ν_{asym}(COO) band is shifted to higher

Table 2 IR assignment (4000–200 cm^{-1}) of HL and its complexes

Compound	ν(C=N)	ρ(py)	ν(C-O)	δ(OH)	ν(C=O)	ν_{asym} (COO)	ν_{sym} (COO)	ν(M O) aliphatic OH	ν(M–O) (ester)	ν(M–N)
HL	1590 sh	667 m	1231 m	1445 m	1732 sh	1573 sh	1304 sh	–	–	–
$[Fe(HL)_2]Cl_2$	1607 sh	669 sh	1250 m	1465 m	1773 m	1576 m	1330 m	550 s	521 s	444 s
$[Fe(HL)_2]Cl_3 \cdot 4H_2O$	1639 m	685 m	1272 m	1400 sh	1756 s	1595 m	1300 m	561 m	489 m	476 s
$[Co(HL)_2]Cl_2$	1599 sh	679 m	1245 sh	1396 m	1678 sh	1570s	1301 sh	530 m	490 s	461 m
$[Ni(HL)Cl_2]\cdot H_2O$	1603 sh	620 m	1277 m	1398 m	1672 sh	1585 m	1306 m	520 s	490 s	469 w
$[Cu(HL)_2]Cl_2$	1607 sh	690 m	1250 sh	1431 m	1738 sh	1580 m	1292 sh	530 s	480 s	456 w
$[Zn(HL)Br_2]$	1607 sh	690 m	1248 m	1433 m	1740 h	1580 m	1323 sh	545 s	490 s	460 w
$[UO_2(HL)_2](NO_3)_2$	1599 sh	679 m	1246 m	1423 m	1680 sh	1570 s	1331 sh	530 s	475 s	462 w

s = small; w = weak; m = medium; br = broad, sh = sharp

wavelengths (1576–1595 cm^{-1}) or lower wavelengths (1570 cm^{-1}), while ν_{sym}(COO) band is shifted to higher wavelengths (1306–1331 cm^{-1}) or lower wavelengths (1301–1300 cm^{-1}). The shift of these two bands to higher or lower frequencies suggest the participation of –COOMe group in complex formation [11, 12]. Coordination of aliphatic OH group can be confirmed by the blue or red shift of ν(C–O) aliphatic and in-plane OH bending δ(OH). The band at 1231 cm^{-1} which is attributed to ν(C–O) in free ligand is shifted to higher frequency (14–46 cm^{-1}), while the band at 1445 cm^{-1} which is attributed to δ(OH) in free ligand is shifted to higher frequencies (20 cm^{-1}) or to lower frequencies (12–49 cm^{-1}) by the effect of the metal complexation. New bands observed in the complexes at 561–520, 521–475 and 476–444 cm^{-1} are tentatively assigned to the ν(M–O) of aliphatic OH, ν(M–O) of ester and ν(M–N) of the pyridine [6, 9].

In the UO_2(II) complex, two additional bands at 950 and 862 cm^{-1}, which are assigned to $\nu_{asym}(UO_2)$ and $\nu_{sym}(UO_2)$ modes, respectively. This observation indicates that the O=U=O moiety is virtually in this complex.

Therefore from the IR spectra, it is obvious that HL ligand behaves as a neutral terdentate ligand coordinated to the metal ions via pyridyl-N, carbonyl ester and protonated aliphatic OH groups.

^{1}H NMR spectra

The ^{1}H NMR spectra of HL and its diamagnetic Zn(II) complex are shown in Fig. 3 and the data are listed in Table 3. It is apparent from the spectra that the aliphatic OH proton signal shifts downfield (3.87 ppm *vs.* 2.96 ppm in the ligand) upon complexation, which confirms the coordination by aliphatic oxygen to the metal ions without deprotonation. This is supported by the IR and molar conductance data. The upfield shifts in the other signals may be due to their affection by the coordination of the pyridyl-N, carbonyl ester and aliphatic-OH to the metal ions.

Table 3 ^{1}H NMR data of HL and its Zn complex

Compound	Chemical shift (δ) ppm	Assignment
HL	7.75	(t, 1H, py, J = 7.3 Hz)
	7.35	(d, 2H, py, J = 7.3 Hz)
	4.65	(s, 2H, $–CH_2$)
	3.94	(s, 3H, $–COOH_3$)
	2.96	(bs, 1H, –OH)
$[Zn(H L)Br_2]$	7.99	(t, 1H, py, J = 7.3 Hz)
	7.39	(d, 2H, py, J = 7.3 Hz)
	4.61	(s, 2H, $–CH_2$)
	4.35	(s, 3H, $–CH_3$)
	3.87	(bs, H, –OH)

Molar conductance data

The observed molar conductance Δ_m=13.75 and 31.42 Ω^{-1} cm^2 mol^{-1} of the Ni(II) and Zn(II) complexes, respectively, in 10^{-3} M DMF solutions are given in Table 1 which suggest the non-electrloytic nature of these complexes [13]. While the molar conductance values (Δ_m=185–202 Ω^{-1} cm^2 mol^{-1}) of the Fe(II), Co(II), Cu(II) and UO_2(II) complexes indicate the electrolytic nature of these complexes and that they are of the type 1:2 electrolytes [13]. The Fe(III) complex has a molar conductance value of 280 Ω^{-1} cm^2 mol^{-1} which indicates that it is a 1:3 electrolyte [13].

Electronic spectra and magnetic moment data

As the result of failer to obtain a single crystal for X-ray analyses to confirm the octahedral and trigonal bipyramidal structures for these complexes, solid

Table 4 Thermal analysis data of the metal chelates

Complex	Temp. range /°C	DTG_{max}/°C	n^*	Mass loss	Total mass loss	Assignment	Metallic residue
				% Found (Calcd)			
$[Fe(HL)_2]Cl_3\cdot 4H_2O$	30–130 130–270 270–600	85 240 465	1.0 1.0 1.0	12.00 (12.66) 20.00 (19.26) 53.00 (53.47)	85.00 (85.39)	-Loss of $4H_2O$ (hydrated). -Loss of 3HCl. -Loss of two ligand molecules.	½Fe_2O_3
$[Ni(HL)Cl_2]\cdot H_2O$	30–110 110–250 250–650	50 165, 210 310, 405, 575	1.0 2.0 3.0	6.00 (5.71) 23.00 (23.18) 48.00 (47.30)	77.00 (76.19)	-Loss of H_2O (hydrated). -Loss of 2HCl. -Loss of ligand molecule.	NiO
$[Cu(HL)_2]Cl_2$	170–220 220–650	205 265, 500	1.0 2.0	15.00 (15.58) 68.00 (67.02)	83.00 (82.60	Loss of 2HCl. -Loss of two ligand molecules.	CuO
$[Zn(HL)Br_2]$	190–450 450–700	220, 320 550	2.0 1.0	41.00 (41.33) 39.00 (38.01)	80.00 (79.34)	-Loss of 2HBr. -Loss of ligand molecule.	ZnO
$[UO_2(HL)_2](NO_3)_2$	70–350 350–800	320 410, 470, 510	1.0 1.0	18.00 (17.13) 46.00 (46.13)	64.00 (63.26)	-Loss of $2NO_2$ and O_2. -Loss of $C_{16}H_{18}N_2O_6$.	UO_2

n^* = number of decomposition steps

Table 5 Thermodynamic data of the thermal decomposition of HL chelates

Complex	Decomp. range/°C	E^*/ kJ mol^{-1}	A/ s^{-1}	ΔS^*/ J K^{-1}mol^{-1}	ΔH^*/ kJ mol^{-1}	ΔG^*/ kJ mol^{-1}	r^2
$[Fe(HL)_2]Cl_3\cdot 4H_2O$	30–130	35.12	$1.01\cdot 10^4$	–18.99	34.42	36.03	0.977
	130–270	37.17	$4.27\cdot 10^5$	–16.29	35.18	39.08	0.979
	270–600	66.29	$3.99\cdot 10^3$	–21.47	62.97	71.56	0.947
$[Ni(HL)Cl_2]\cdot H_2O$	30–110	13.03	9.22	–25.46	12.61	13.89	0.897
	110–250	45.10	$1.64\cdot 10^7$	–12.39	43.54	45.87	0.952
	250–650	29.69	2.94	–28.76	26.12	38.49	0.956
$[Cu(HL)_2]Cl_2$	170–220	144.5	$1.35\cdot 10^{15}$	–5.75	142.8	141.6	0.959
	220–650	26.27	1.14	–29.58	23.09	34.39	0.931
$[Zn(HL)Br_2]$	190–450	132.2	$3.99\cdot 10^{12}$	–0.35	129.9	130.0	0.931
	450–700	79.90	$4.39\cdot 10^2$	–21.70	75.32	87.26	0.942
$[UO_2(HL)_2](NO_3)_2$	70–350	2.15	$4.69\cdot 10^{-1}$	–30.29	0.52	9.18	0.947
	350–800	7.55	$1.24\cdot 10^1$	–27.34	3.89	15.92	0.955

reflectance spectra and magnetic moment measurements are used for this purpose.

The solid reflectance spectra of the complexes show three bands in the range 46.269–43.478, 41.666–39.682 and 33.333–32.362 cm^{-1} which may attribute to interligand transitions.

The diffused reflectance spectrum of Fe(II) complex displays two absorption bands at 12.820 and 20.000 cm^{-1} which are assigned to $^5T_{2g}\longrightarrow{}^5E_g$ transition and charge transfer, respectively [14, 15]. It exhibits magnetic moment values of 4.98 B.M., which are consistent with a high spin octahedral geometry.

In the high spin octahedral Fe(III) complex, the magnetic moment is always very close to spin-only value of 5.9 B.M. because the ground state has no orbital angular momentum. The complex under study has a magnetic moment of 5.30 B.M.; where Fe(III) has the ground state ^6S. Reflectance spectrum shows three bands at 21.321, 17.452 and 12.820 cm^{-1} which may be assigned to $^6A_{1g}\rightarrow T_{2g}$ (G) transition in octahedral geometry [16]. Also the spectrum shows a band at 23.255 cm^{-1} which can be attributed to charge transfer.

The electronic spectra of Co(II) complex give three bands at 12.738, 15.082 and 17.482 cm^{-1} . The fourth band at 22.624 cm^{-1} refers to the charge transfer band. The bands observed are assigned to the transitions $^4T_{1g}$ (F) $\longrightarrow$ $^4T_{2g}$ (F) (ν_1), $^4T_{1g}$ (F)$\longrightarrow$$^4A_{2g}$ (F) (ν_2) and $^4T_{1g}$ (F)$\longrightarrow$$^4T_{2g}$ (P) (ν_3), respectively, suggesting that there is an octahedral geometry around Co(II) ion [17–19].

For calculating the Racah parameters, the following two equations are used [18].

$$10Dq= 2\nu_1-\nu_3 + 15B$$

$$B=1/30\ [-(\nu_1-\nu_3)\pm(-\nu_1^2 + \nu_3^2 +\nu_1\nu_3)^{1/2}]$$

$$10Dq=1/3\ (2\nu_2-\nu_3)+5B$$

$$B=1/510\ \{7\ (\nu_3-2\nu_2)\pm3\ [81\nu_3^2-16\nu_2\ (\nu_2-\nu_3)^{1/2}]\}$$

From the position of the bands and the calculated Racah parameters, the chelates are octahedral with largely covalent bonds between the organic ligands and the metal ion [18]. The magnetic susceptibility measurement lie at 5.15 B.M. range (normal range for octahedral Co(II)–complexes is 4.3–5.2 B.M.), is an indicative of octahedral geometry [20].

The reflectance spectrum of Cu(II) chelate shows broad band at 22.935 cm^{-1} that forms part of the charge transfer band. The ^2E_g and $^2T_{2g}$ states of the octahedral copper(II) ion (d^9) split under the influence of the tetragonal distortion and the distortion can be such as to cause the three transitions $^2B_{1g}\rightarrow{}^2B_{2g}$; $^2B_{1g}\rightarrow{}^2E_g$ and $^2B_{1g}\rightarrow{}^2A_{1g}$ to remain unresolved in the spectra [21]. It is concluded that, all three transitions lie within the single broad envelope centered at 17.421 cm^{-1}. This assignment is in agreement with the general observation that copper(II) *d–d* transitions are normally close in energy [22]. The magnetic moment value of 1.95 B.M. falls within the range normally observed for octahedral Cu(II) complexes [23].

The reflectance spectrum of the Ni(II) complex shows recognizable spectral bands at 13.157, 17.361 and 21.691 cm^{-1}. The positions of these spectral bands are quite consistent with those predicted for five coordinate Ni(II) complex whose structure has been established by X-ray crystallographic measurements [24].

The bands can be assigned respectively [24] to $^3B_1\rightarrow{}^3E$, $^3B_1\rightarrow{}^3A_2$ and $^3B_1\rightarrow{}^3E$ transitions assuming the effective symmetry to be C_{4V}. The band at 29.069 cm^{-1} may assign to L- M CT band.

The Zn(II) and UO_2(II) complexes are diamagnetic and assumed respectively to be trigonal bipyramidal and octahedral structures.

Thermal analysis data

The thermal decomposition curves are given for Fe(III), Zn(II) and UO_2(II) complexes, as examples, are represented graphically in Fig. 4. The thermogravimetric analysis of the complexes was recorded in the 30–800°C range. The Fe(III) and Ni(II) complexes show the same decomposition pattern. The Fe(III) complex decompose in three steps while the Ni(II) complex decompose in five steps. The first step is related to the evolution of hydrated water molecules ($4H_2O$:13.00, calcd. 12.66% for Fe(III) complex; H_2O:found 6.00%, calcd. 5.71% for Ni(II) complex) leaving anhydrous complexes. The anhydrous complexes decompose in the subsequent steps within the temperature range 110–650°C leaving $½Fe_2O_3$ and NiO residues.

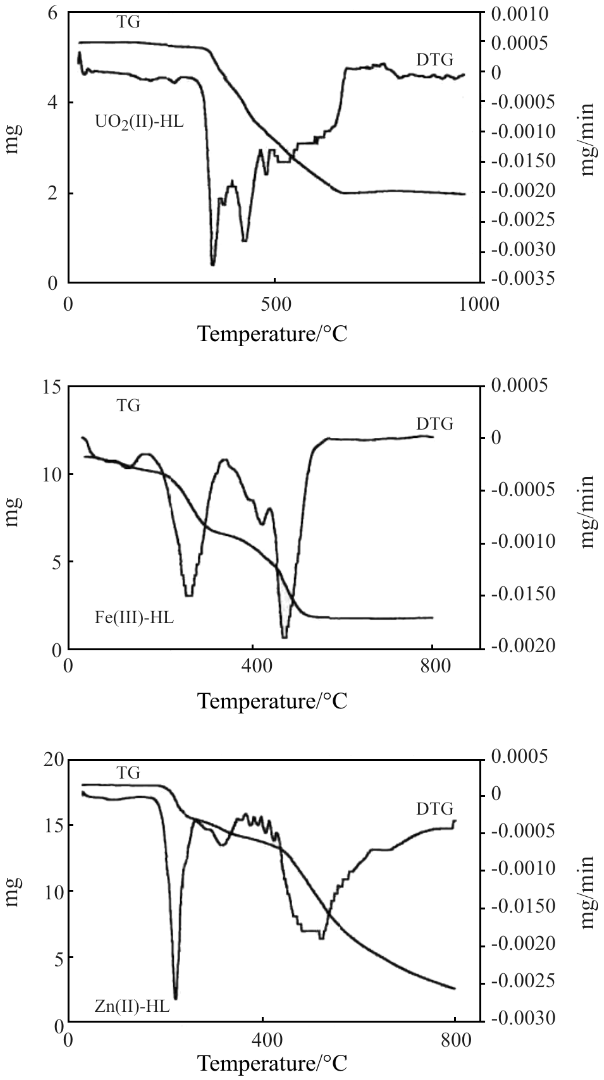

Fig. 4 TG and DTG plots of UO_2(II), Fe(III) and Zn(II) complexes

The TG curves of the Cu(II), Zn(II) and UO_2(II) complexes consist of two or three stages of mass loss. The first and first and second mass loss occur in the range 70–450°C can be attributed to a loss of HBr, HCl, $2NO_2$ and O_2 gases. The final step within the temperature range 220–800°C corresponds to the decomposition of the ligand molecules as CO_2, NO_2, NO, CO, O_2,…etc gases with an estimated mass loss of 68.00 (calcd. 67.02%), 39.00% (calcd. 38.01%) and 46.00% (calcd. 46.13%) for the Cu(II), Zn(II) and UO_2(II) complexes, respectively. The final products for these decomposition are CuO, ZnO and UO_2 residues.

Kinetic parameters of the complexes

The kinetic parameters namely activation energy (E^*), enthalpy (ΔH^*), entropy (ΔS^*) and free energy change of decomposition (ΔG^*) were evaluated graphically by employing the Coats–Redfern relation [25]:

$$\log[\log[W_{\mathrm{f}} / (W_{\mathrm{f}} - W)] / T^{2}] = \log[AR / E^{*}(1 - 2RT / E^{*})] - E^{*} / 2.303RT \quad (1)$$

where W_f is the mass loss at the completion of the reaction, W is the mass loss up to the temperature T, R is the gas constant, E^* is the activation energy in kJ mol^{-1}, θ is the heating rate and $(1-(2RT)E^*))\cong 1$. A plot of the left-hand side of Eq.(1) *vs.* $1/T$ gives a slope from which E^* was calculated and A (Arrhenius constant) was determined from the intercept. The entropy of activation (ΔS^*), enthalpy of activation (ΔH^*) and free energy change of activation (ΔG^*) were calculated using the following equations:

$$\Delta S^* = 2.303[\log(Ah/kT)]R \quad (2)$$

$$\Delta H^* = E^* - RT \quad (3)$$

$$\Delta G^* = \Delta H^* - T\Delta S^* \quad (4)$$

where k and h are the Boltzman and Plank constants, respectively.

For all the complexes studied, the activation energies of the decomposition steps are recorded in Table 5. The activation energy of the dehydration of the Fe(III) and Ni(II) complexes is found to be 35.12 and 13.03 kJ mol^{-1}. In addition, the activation energies of the elimination of the anions in all the complexes are shown in the range 2.15–144.47 kJ mol^{-1}. Moreover, the activation energies for the removal of the ligand molecules in all the complexes are found to be 7.35–79.90 kJ mol^{-1}. The thermodynamic parameter data are listed in Table 5 from which it is obvious that all the complexes have negative entropy values, which indicates that the activated complexes are formed spontaneously.

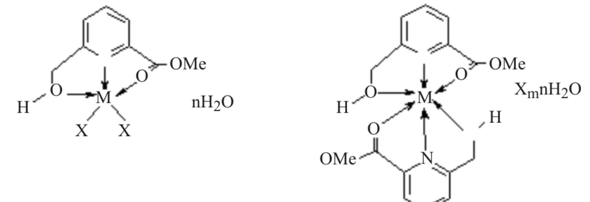

M= Ni(II), X=Cl, n=1
Zn(II), X=Br, n=0

M= Fe(II), X=Cl, m=2, n=1
Fe(III), X=Cl, m=3, n=4
Co(II), X=Cl, m=2, n=0
Cu(II), X=Cl, m=2, n=0
UO_2(II), X=NO_3, m=2, n=0

Fig. 5 Suggested structural formulas of HL complexes

Structural interpretation

From the above data, the structure of the complexes can be given as shown in Fig. 5.

Conclusions

From the satisfactory microanalytical, magnetic, molar conductance and various spectral data, it is concluded that HL acts as a neutral terdentate ligand and coordinate through its aliphatic OH (protonated), pyridyl-N and carbonyl ester atoms to yield five- and six-coordinate metal complexes. The thermoanalytical results of the complexes conclusively prove that the hydrated water and anions are removed in the first steps followed immediately by decomposition of the ligand molecules. Also, the metal oxides; ½Fe_2O_3, NiO, CuO, ZnO and UO_2 are the final products.

References

1 A. J. Canty and G. Van Koten, Acc. Chem. Res., 28 (1995) 406.
2 R. A. T. M. Abbenhuis, I. Del Rio, M. M. Bergshoef, J. Boesma, A. L. Speck and G. Van Koten, Inorg. Chem., 37 (1998) 1749.
3 I. Del Rio, R. A. Gossage, M. S. Hannu, M. Lutz, A. L. Speck and G. Van Koten, Organometallics, 18 (1999) 1097.
4 G. G. Mohamed and N. E. A. El-Gamel, Spectrochim. Acta, (Part A) 61 (2005) 1089.
5 C. Gemel, K. Foltin and G. K. Caulton, Inorg. Chem., 39 (2000) 1593.
6 G. G. Mohamed, N. E. A. El-Gamel and F. Teixidor, Polyhedron, 20 (2001) 2689.
7 D. X. West, J. K. Swearingen, J. V. Martinez, S. H. Ortega, A. K. El-Sawaf, F. V. Meurs, A. Castineiras, I. Garcia and E. Bermejo, Polyhedron, 18 (1999) 2919.
8 K. Nakamoto, 'Infrared and Raman Spectra of Inorganic and Coordination Compounds', Wiley, New York, 4th Edn., 1980.
9 G. G. Mohamed, F. A. N. El-Dien and N. E. A. El-Gamel, J. Therm. Anal. Cal., 67 (2002) 135.
10 T. Miyazawa, T. Shimanouchi and S. Mizushima, J. Chem. Phys., 29 (1958) 611.
11 N. Rao, P. V. Rao, V. Raju and M. C. Ganorkar, Indian J. Chem., 24A (1985) 877.
12 G. K. Sandhu and S.P. Verma, Polyhedron, 6 (1987) 587.
13 J. A. Dean, Lange's Handbook of Chemistry, Ed., 14th Edition, New York, MC Graw – Hill, Table 8.35, 1992.
14 F. A. Cotton, G. Wilkinson, C. A. Murillo and M. Bochmann, Advanced Inorganic Chemistry, 6th Edn., Wiley, New York, 1999.
15 A. Hazell, C. J. Mckenzie and L. P. Nielsen, Polyhedron, 19 (2000) 1333.
16 M. M. Moustafa, J. Thermal Anal., 50 (1997) 463.
17 G. G. Mohamed and Z. H. Abd El-Wahab, J. Therm. Anal. Cal., 73 (2003) 347.
18 M. S. Masoud, A. M. Hindawy and A. S. Soayed, Trans. Met. Chem., 16 (1991) 372.
19 N. K. Gaur, R. Sharma and R. S. Sindhu, J. Indian Chem. Soc., 78 (2001) 26.
20 N. Mondal, D. K. Dey, S. Mitra and K. M. Abdul Malik, Polyhedron, 19 (2000) 2707.

21 J. Kohout, M. Hvastijova, J. Kozisek, J. G. Diaz, M. Valko, L. Jager and I. Svoboda, Inorg. Chim. Acta, 287 (1999) 186.

22 A. Bury, A. E. Underhill, D. R. Kemp, N. J. O'shea, J. P. Smith and P. S. Gomm, Inorg. Chim. Acta, 138 (1987) 85.

23 N. R. S. Kumar, M. Nethiji and K. C. Patil, Polyhedron, 10 (1991) 365.

24 N. Saha, J. Ind. Chem. Soc., 69 (1992) 517 and references therein.

25 A. W. Coats and J. P. Redfern, Nature, 20 (1964) 68.

Received: September 7, 2004
In revised form: December 6, 2004

DOI: 10.1007/s10973-005-6428-y